The Measurement of Incident and Reflected Spectra Using a Least Squares Method

by

E.P.D. Mansard* and E.R. Funke**

ABSTRACT

A least squares method to separate the incident and reflected spectra from the measured co-existing spectra is presented. This method requires a simultaneous measurement of the waves at three positions in the flume which are in reasonable proximity to each other and are on a line parallel to the direction of wave propagation.

Experimental investigations have shown that there is good agreement between the incident spectra calculated by the least squares method and the incident spectra measured concurrently in a side channel.

1.0 INTRODUCTION

As a large number of hydraulic laboratories now have the capability of generating irregular sea states for their experimental investigations, the necessity for computing reflections in an irregular sea state has become urgent. The presently available technique for this purpose is a 2-point method advanced by Thornton and Calhoun (1972), Goda and Suzuki (1976), and Morden et al (1976), which consists of measuring simultaneously the co-existing wave spectra at two known positions on a line parallel to the direction of wave propagation and deriving from this the incident and reflected spectra. This method has, however, certain limitations.

This paper presents a 3-point method which uses a least square analysis for decomposing the measured spectra into incident and reflected spectra with greater accuracy and range. This method originally derived by Marcou (1969) was used extensively for reflections with periodic waves (Mansard, 1976) and yielded reliable results.†

Assistant* and Senior** Research Officers, Hydraulics Laboratory, National Research Council of Canada, Ottawa.

† A recently proposed method by Gaillard et al (1980) also employs a 3-point measurement and contains some similarity to the method described here.

Downloaded from ascelibrary.org by "University of California, San Diego" on 11/17/20. Copyright ASCE. For personal use only; all rights reserved.

Downloaded from ascelibrary.org by "University of California, San Diego" on 11/17/20. Copyright ASCE. For personal use only; all rights reserved.

This paper describes the extension of this method to irregular waves and presents some experimental results obtained with a rubble mound breakwater.

2.0 REFLECTION MEASUREMENTS FOR IRREGULAR WAVES

The main assumption underlying the analysis of reflections in an irregular sea state is that the irregular waves can be described as a linear superposition of an infinite number of discrete components each with their own frequency, amplitude and phase. Another assumption, which is also of importance, is that these components travel at their own individual phase velocities described by the dispersion relationship. The first assumption is a widely accepted axiom in irregular wave studies while the second one has been found, through experimental investigations, to be a qood approximation for finite and infinite depths of water (Funke and Mansard, 1980).

2.1 The 2-point Method

This method consists of measuring simultaneously the co-existing waves (two progressive wave trains moving in opposite direction) at two known positions in the flume, in a line parallel to the direction of wave propagation. Fourier analysis of these two signals will then produce the amplitudes and phases of the wave components at these two positions, by means of which the standing wave can be resolved into incident and reflected waves. This method described in detail by Thornton et al (1972) and Goda et al (1976) was developed by applying linear wave theory to monochromatic waves.

The above 2-point method has, however, certain limitations:

1. Limited Frequency Range
   a) If the spacing between the probes is too great, the coherency factor which estimates the relative phase stability in each spectral frequency band decreases as the frequency increases, thus making the calculations of reflections less reliable.
   b) If the spacing is too short, then there is a loss of contrast in cross spectral analysis.
2. Critical Probe Spacing
   If the probe spacing "x" is such that $x/L = n/2$ ($n=0,1,2 \ldots$, L = wave length), the values of reflections become indeterminate because the proposed equa-

Downloaded from ascelibrary.org by "University of California, San Diego" on 11/17/20. Copyright ASCE. For personal use only; all rights reserved.

tions have singularities at these values.

3. High sensitivity to errors in the measurement of waves due to:
   a) Transversal waves in the flume,
   b) Non-linear wave interactions,
   c) Harmonics due to non-linearities,
   d) Signal noise, measurement errors, etc.

In order to overcome the above limitations, a 3-point method using a least squares method was developed.

2.2.1 The Least Squares Method

A definition sketch for this analysis is presented in Fig. 1.

Let us assume that waves are travelling in a channel in a longitudinal direction and reflections from some arbitrary structure or beach are travelling in the opposite direction. Assume also that it is possible to measure simultaneously the linear superpositions of these waves at m points p = 1, 2, 3 to m, which are in reasonable proximity to each other and are on a line parallel to the direction of wave propagation.

The wave profile observed at any one of these probe positions may be given as a summation of discrete, harmonically related Fourier components, i.e.

$$\eta_p(t) = \sum_{k=1}^{N} A_{p,k} \cdot \sin\left(\frac{2\pi \cdot k \cdot t}{T} + \alpha_{p,k}\right) \qquad (1)$$

where $A_{p,k}$ is the Fourier coefficient for frequency k/T,
T is the length of the wave profile which is being observed; thus the fundamental frequency is $f_0 = 1/T$,
$\alpha_{p,k}$ is the phase relative to the time origin of the record,
N is an upper limit of summation which depends on the maximum significant frequency component in the series.

The Fourier coefficients and their phases are obtained from a Fourier transform of the function

$$\eta_p(t), \qquad 0 \leq t \leq T \qquad (2)$$

and are given in polar form as:

$$B_{p,k} = A_{p,k} \cdot e^{i\alpha_{p,k}} \qquad (3)$$

Downloaded from ascelibrary.org by "University of California, San Diego" on 11/17/20. Copyright ASCE. For personal use only; all rights reserved.

or in rectangular form as:

$$B_{p,k} = [A_{p,k} \cdot \cos(\alpha_{p,k}) + i \cdot A_{p,k} \cdot \sin(\alpha_{p,k})] \quad (4)$$

Since the spacing between the various probes is known and since it is established that (except for locked harmonics) individual frequency components in a composite wave train travel at their own celerity (Funke and Mansard, 1980; Goda and Suzuki, 1976), it is possible to calculate the phase relationships between the wave trains as observed by each of the three probes. The general equation for a progressive wave is:

$$\eta_x(t) = \sum_{k=1}^{N} C_k \cdot \sin\left(-\frac{2\pi \cdot k \cdot t}{T} + \frac{2\pi x}{L_k} + \theta_k\right) \quad (5)$$

where θ_k is some arbitrary phase related to the space and time origin of the function,
x is a space variable measured from the space origin of the function in a direction of wave propagation,
L_k is the wave length of frequency k/T.

The observation of wave activity made at point p can now be stated in terms of a summation of

a) an incident wave $C_{I,k}$
b) a reflected wave $C_{R,k}$
c) a noise signal which may be caused due to
   - cross-nodal activity
   - locked harmonics
   - non-linear interactions
   - measurement errors.

Let the distance from the wave source to the probe at p=1 be X1 and let the distance from the probe at p=1 to the reflecting structure be XR1, then the wave profile as observed at the probe may be written as:

$$\eta_{p=1}(t) = \sum_{k=1}^{N} C_{Ik} \cdot \sin\left(-\frac{2\pi \cdot k \cdot t}{T} + \frac{2\pi \cdot X1}{L_k} + \theta_k\right) + \sum_{k=1}^{N} C_{Rk} \cdot \sin\left(-\frac{2\pi \cdot k \cdot t}{T} + \frac{2\pi \cdot (X1+2 \cdot XR1)}{L_k} + \theta_k + \phi_k\right) + \Omega_1(t) \quad (6)$$

Downloaded from ascelibrary.org by "University of California, San Diego" on 11/17/20. Copyright ASCE. For personal use only; all rights reserved.

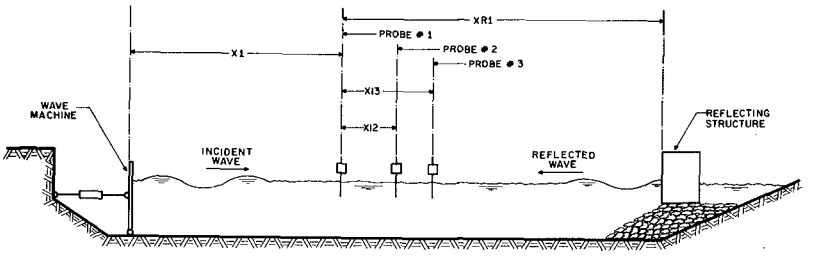

FIG. 1
SET-UP FOR WAVE REFLECTION MEASUREMENT

where $\Omega_1(t)$ is the cumulative effect of all the corrupting signals at probe p=1 and ϕ_k is a phase change due to the reflecting structure. The second probe at p=2, which is displaced by a distance X12 from the probe at p=1 in the direction of incident wave propagation (see Fig. 1), will record a similar wave profile as Eq. 6 except the phase angles will now be

$$\left(-\frac{2\pi \cdot k \cdot t}{T} + \frac{2\pi \cdot (X1+X12)}{L_k} + \theta_k\right) \tag{7}$$

for the incident wave and

$$\left(-\frac{2\pi \cdot k \cdot t}{T} + \frac{2\pi \cdot (X1 + 2 \cdot XR1 - X12)}{L_k} + \theta_k + \phi_k\right) \tag{8}$$

for the reflected wave. A similar argument will define the wave angles for other probe positions which are displaced by distances X1P from the first probe.

Fourier transformation of the composite signal, as

described by Eq. 6, over the interval $0 < t < T$ yields:

$$F[\eta_{p=1}(t)] = B_{1,k} = C_{I,k}\cdot\exp\left(i\cdot\frac{2\pi\cdot X1}{L_k} + i\cdot\theta_k\right) + C_{R,k}\cdot\exp\left(i\cdot\frac{2\pi\cdot(X1+2\cdot XR1)}{L_k} + i(\theta_k+\phi_k)\right) + Y_{1,k}\cdot\exp\cdot i(\rho_{1,k}) \quad (9)$$

where $\exp(\alpha) = e^{\alpha}$.
Similarly the observed signal for the other probes can be given in terms of their Fourier transforms as:

$$F[\eta_p(t)] = B_{p,k} = C_{I,k}\cdot\exp\left(i\cdot\frac{2\pi\cdot(X1+X1P)}{L_k} + i\cdot\theta_k\right) + C_{R,k}\cdot\exp\left(i\cdot\frac{2\pi\cdot(X1+2\cdot XR1-X1P)}{L_k} + i(\theta_k+\phi_k)\right) + Y_{p,k}\cdot\exp\cdot i(\rho_{p,k}) \quad (10)$$

Since one is only interested in the phase differences between the various probes, Eqs. 9 and 10 may be simplified in such a manner that the relevant phase differences are revealed. Therefore, let:

$$Z_{I,k} = C_{I,k}\cdot\exp\left(i\cdot\frac{2\pi\cdot X1}{L_k} + i\cdot\theta_k\right)$$

$$Z_{R,k} = C_{R,k}\cdot\exp\left(i\cdot\frac{2\pi\cdot(X1+2\cdot XR1)}{L_k} + i(\theta_k+\phi_k)\right) \quad (11)$$

$$Z_{N,p,k} = Y_{p,k}\cdot\exp\cdot i(\rho_{p,k})$$

Consequently one obtains for the first three probes:

$$B_{1,k} = Z_{I,k} + Z_{R,k} + Z_{N,1,k} \quad (12)$$

$$B_{2,k} = Z_{I,k}\cdot\exp\left(i\cdot\frac{2\pi\cdot X12}{L_k}\right) + Z_{R,k}\cdot\exp\left(-i\cdot\frac{2\pi\cdot X12}{L_k}\right) + Z_{N,2,k} \quad (13)$$

$$B_{3,k} = Z_{I,k}\cdot\exp\left(i\cdot\frac{2\pi\cdot X13}{L_k}\right) + Z_{R,k}\cdot\exp\left(-i\cdot\frac{2\pi\cdot X13}{L_k}\right) + Z_{N,3,k} \quad (14)$$

Downloaded from ascelibrary.org by "University of California, San Diego" on 11/17/20. Copyright ASCE. For personal use only; all rights reserved.

Downloaded from ascelibrary.org by "University of California, San Diego" on 11/17/20. Copyright ASCE. For personal use only; all rights reserved.

The Z_N terms cannot be measured, but for the purpose of solving for Eqs. 12, 13 and 14, a least squared error method may be employed as follows:

For convenience define

$$\psi_{p,k} = \frac{2\pi \cdot X1P}{L_k} \tag{15}$$

where X1P is the distance between probe 1 and probe 'p'.

In particular let

$$\beta_k = \psi_{2,k} = \frac{2\pi \cdot X12}{L_k}$$
$$\gamma_k = \psi_{3,k} = \frac{2\pi \cdot X13}{L_k} \tag{16}$$

Eqs. 12 to 14 may now be restated thus:

$$\begin{aligned} Z_{I,k} + Z_{R,k} - B_{1,k} &= \varepsilon_{1,k} \\ Z_{I,k} \cdot e^{i\beta k} + Z_{R,k} \cdot e^{-i\beta k} - B_{2,k} &= \varepsilon_{2,k} \\ Z_{I,k} \cdot e^{i\gamma k} + Z_{R,k} \cdot e^{-i\gamma k} - B_{3,k} &= \varepsilon_{3,k} \end{aligned} \tag{17}$$

where

$$\varepsilon_{p,k} = -Z_{N,p,k} + f_e(Z_{I,k}, Z_{R,k}) \tag{18}$$

By applying a least squares method one may find those values of Z_I and Z_R for which the sum of squares of $\varepsilon_{p,k}$ for all 'p' is minimum. This should correspond to those values of $Z_{I,k}$ and $Z_{R,k}$ for which

$$f_e(Z_{I,k}, Z_{R,k}) = 0.$$

Downloaded from ascelibrary.org by "University of California, San Diego" on 11/17/20. Copyright ASCE. For personal use only; all rights reserved.

It is therefore required that

$$\sum_{p=1}^{3} (\varepsilon_{p,k})^2 = \sum_{p=1}^{3} \left(Z_{I,k} \cdot e^{i\psi_{p,k}} + Z_{R,k} \cdot e^{-i\psi_{p,k}} - B_{p,k} \right)^2 \qquad (19)$$

= a minimum.

It is assumed that this minimum is reached when both partial derivatives are zero, i.e.

$$\frac{d\left(\sum_{p=1}^{3} (\varepsilon_{p,k})^2 \right)}{d\, Z_{I,k}} = \frac{\left(\sum_{p=1}^{3} (\varepsilon_{p,k})^2 \right)}{d\, Z_{R,k}} = 0 \qquad (20)$$

Differentiating Eq. 19, one therefore obtains:

$$\sum_{p=1}^{3} \left(Z_{I,k} \cdot e^{i\psi_{p,k}} + Z_{R,k} \cdot e^{-i\psi_{p,k}} - B_{p,k} \right) \cdot e^{i\psi_{p,k}} = 0 \qquad (21)$$

and

$$\sum_{p=1}^{3} \left(Z_{I,k} \cdot e^{i\psi_{p,k}} + Z_{R,k} \cdot e^{-i\psi_{p,k}} - B_{p,k} \right) \cdot e^{-i\psi_{p,k}} = 0 \qquad (22)$$

Eqs. 21 and 22 may now be written as follows:

$$Z_{I,k} \cdot \left(1 + e^{i \cdot 2 \cdot \beta_k} + e^{i \cdot 2 \cdot \gamma_k} \right) + 3\, Z_{R,k} = B_{1,k} + B_{2,k} \cdot e^{i\beta_k} + B_{3,k} \cdot e^{i \cdot \gamma_k} \qquad (23)$$

$$Z_{R,k} \cdot \left(1 + e^{-i \cdot 2 \cdot \beta_k} + e^{-i \cdot 2 \cdot \gamma_k} \right) + 3\, Z_{I,k} = B_{1,k} + B_{2,k} \cdot e^{-i \cdot \beta_k} + B_{3,k} \cdot e^{-i \cdot \gamma_k} \qquad (24)$$

where β and γ were defined by Eq. 16. From these, the solu-

Downloaded from ascelibrary.org by "University of California, San Diego" on 11/17/20. Copyright ASCE. For personal use only; all rights reserved.

tions for Z_I and Z_R may be derived, namely:

$$Z_{I,k} = \frac{1}{D_k} \cdot \left(B_{1,k} \cdot (R1 + i \cdot Q1) + B_{2,k} \cdot (R2 + i \cdot Q2) + B_{3,k} \cdot (R3 + i \cdot Q3) \right) \quad (25)$$

and

$$Z_{R,k} = \frac{1}{D_k} \cdot \left(B_{1,k} \cdot (R1 - i \cdot Q1) + B_{2,k} \cdot (R2 - i \cdot Q2) + B_{3,k} \cdot (R3 - i \cdot Q3) \right) \quad (26)$$

where:

$$\begin{aligned} D_k &= 2 \cdot (\sin^2\beta_k + \sin^2\gamma_k + \sin^2(\gamma_k - \beta_k)) \\ R1_k &= \sin^2\beta_k + \sin^2\gamma_k \\ Q1_k &= \sin\beta_k \cdot \cos\beta_k + \sin\gamma_k \cdot \cos\gamma_k \\ R2_k &= \sin\gamma_k \sin(\gamma_k - \beta_k) \\ Q2_k &= \sin\gamma_k \cdot \cos(\gamma_k - \beta_k) - 2 \cdot \sin\beta_k \\ R3_k &= -\sin\beta_k \sin(\gamma_k - \beta_k) \\ Q3_k &= \sin\beta_k \cdot \cos(\gamma_k - \beta_k) - 2 \cdot \sin\gamma_k \end{aligned} \quad (27)$$

2.2.2 Analysis Technique

The two equations (25 and 26) are solved independently for each frequency component (using the Fourier transform technique) or for each frequency band (using the technique of spectral analysis by the method of averaged periodogram) and then squared and scaled to give the incident and reflected spectra.

The parameters D_k, $R_{1,k}$, $R_{2,k}$, $R_{3,k}$, $Q_{1,k}$, $Q_{2,k}$ and $Q_{3,k}$ can be obtained easily from the trigonometric relations of the probe spacings. The characteristics of the co-existing wave profiles $B_{p,k}$ which can be expressed as:

$$B_{p,k} = [A_{p,k} \cdot \cos(\alpha_{p,k}) + i \cdot A_{p,k} \cdot \sin(\alpha_{p,k})] \quad (28)$$

are given by one of the above two techniques. The values of $A_{p,k}$ and $\alpha_{p,k}$ can be calculated directly from the Fourier transform, while in the case of spectral analysis they are

obtained by auto and cross spectral density analysis respectively.

By applying a suitable averaging window for spectral density analysis, a representative value of $B_{p,k}$ for each frequency band rather than for every frequency component is obtained. This technique significantly reduces the erratic variations of the reflection coefficient spectrum and, at the same time, reduces the computational task.

The different steps involved in calculating the solutions for the above Eqs. 25 and 26 are described below:

1. The outputs from the three probes are denoted as $\eta_1(t)$, $\eta_2(t)$ and $\eta_3(t)$. Execute auto-spectral density analysis on each record, yielding:

   $$S1(k\cdot\Delta f),\ S2(k\cdot\Delta f) \text{ and } S3(k\cdot\Delta f)$$

   Apply band-limiting, if required and provide spectral smoothing to obtain reliable estimates for each frequency bandwidth.

2. From the auto-spectra compute the amplitude spectra as follows:

   $$A1(k\cdot\Delta f) = \sqrt{2\cdot S1(k\cdot\Delta f)\cdot\Delta f} \qquad (29)$$

   and similarly for A2 and A3.

3. Obtain the cross-spectral density in polar form for $\eta_1(t)$ with $\eta_2(t)$ and $\eta_1(t)$ with $\eta_3(t)$. Apply band-limiting and smoothing identical to that applied under (1).

4. From the cross-spectra, extract the phase spectra

   $$PH12(k\cdot\Delta f) \text{ and } PH13(k\cdot\Delta f)$$

   Also set $PH11(k\cdot\Delta f) = 0$ for all k.

5. Pair up the amplitude and the phase spectra in polar form as follows:

   $A1(k\cdot\Delta f)$ with $PH11(k\cdot\Delta f)$
   $A2(k\cdot\Delta f)$ with $PH12(k\cdot\Delta f)$
   $A3(k\cdot\Delta f)$ with $PH13(k\cdot\Delta f)$

6. Convert from polar to rectangular form so that

   $$B1(k\cdot\Delta f) = REC\{A1(k\cdot\Delta f)\cdot\exp(PH11(k\cdot\Delta f))\}$$

   etc.

Downloaded from ascelibrary.org by "University of California, San Diego" on 11/17/20. Copyright ASCE. For personal use only; all rights reserved.

7. For all k evaluate the angles $\beta(k\cdot\Delta f)$ and $\gamma(k\cdot\Delta f)$ as per Eq. 16. The wave length L_k must be evaluated in terms of the depth of water which may be considered average for the region in which the probes are located.

8. For all k evaluate all the terms of the set of Eq. 27.

9. Evaluate $Z_I(k\cdot\Delta f)$ and $Z_R(k\cdot\Delta f)$ according to Eqs. 25 and 26.

10. From Z_I and Z_R compute the spectral densities S_I and S_R by

$$S_I(k\cdot\Delta f) = |Z_I(k\cdot\Delta f)|^2/(2\cdot\Delta f)$$
and
$$S_R(k\cdot\Delta f) = |Z_R(k\cdot\Delta f)|^2/(2\cdot\Delta f)$$

11. The reflection coefficient is then evaluated from

$$R(k\cdot\Delta f) = |Z_R(k\cdot\Delta f)|/|Z_I(k\cdot\Delta f)|$$

12. The coherency factor should also be computed in order to evaluate the degree of significance of the incident and the reflected spectrum. Thus

$$CF12(k\cdot\Delta f) = |S12(k\cdot\Delta f)|/(S1(k\cdot\Delta f)\cdot S2(k\cdot\Delta f))^{1/2}$$
and
$$CF13(k\cdot\Delta f) = |S13(k\cdot\Delta f)|/(S1(k\cdot\Delta f)\cdot S3(k\cdot\Delta f))^{1/2}$$

3.0 EXPERIMENTAL SET-UP AND TEST RESULTS

Experimental investigations were carried out to determine the reflective characteristics of a rubble mound breakwater subject to irregular wave action. The set-up used for this purpose (Fig. 2) consists of a flume of dimensions 67 m x 1.8 m x 1.25 m, equipped with a hydraulically driven random wave generator. This wave generator, controlled by an on-line computer, can reproduce a variety of simulated natural sea states in the flume (Funke et al, 1980; Funke and Mansard, 1979).

As shown in Fig. 2, the width of the flume was subdivided into three sections: a centre channel of 0.9 m wide and two side channels of 0.45 m wide. The breakwater was placed in the centre channel while beaches with a mild slope of 1:20 ensured a good dissipation of the incident wave energy in the side channels. This particular set-up reduced the secondary reflections from the wave board since half of the secondary reflections were dissipated in the side channels.

Downloaded from ascelibrary.org by "University of California, San Diego" on 11/17/20. Copyright ASCE. For personal use only; all rights reserved.

Downloaded from ascelibrary.org by "University of California, San Diego" on 11/17/20. Copyright ASCE. For personal use only; all rights reserved.

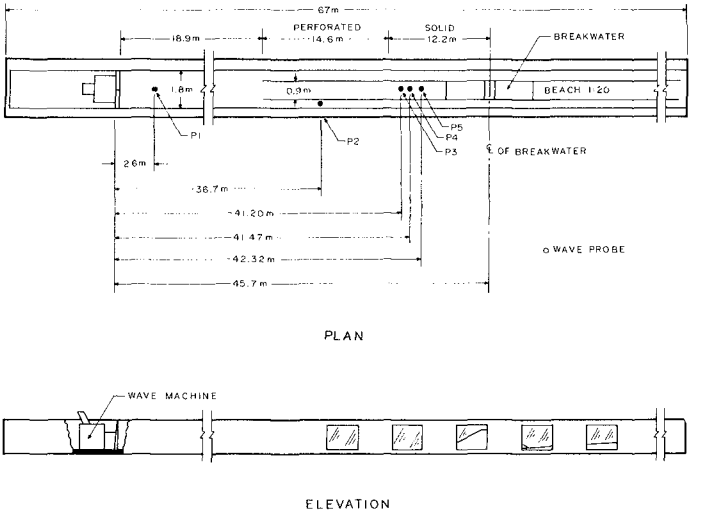

FIG. 2 WAVE FLUME WITH PROBE LOCATIONS

The primary reflections in the side channels being very small (lower than 5% for long waves), the waves therein were considered more or less as pure incident waves. This allowed a direct comparison between the calculated and the actual incident wave spectra.

The waves were sampled simultaneously by the on-line computer at four probe positions (three in the central channel and one in the side channel). The probes used for this purpose are a variation of the Robertshaw capacitance probe which has proved to be quite reliable. The sampling of data, which was initiated only after the reflections had stabilized, was carried out for at least one cycle length of the time series (about 200 s in the model).

Tests were carried out using JONSWAP spectra and the results corresponding to two different peak frequencies are presented below in Figs. 3 and 4. Additional examples can be found in Mansard and Funke (1980).

These results show that the co-existing spectra measured at the three probe positions differ to a certain extent; the values of their characteristic wave height (H_{m0}) and their maximum wave height ($H_{z,max}$) vary. These variations, which could be attributed to the standing wave pat-

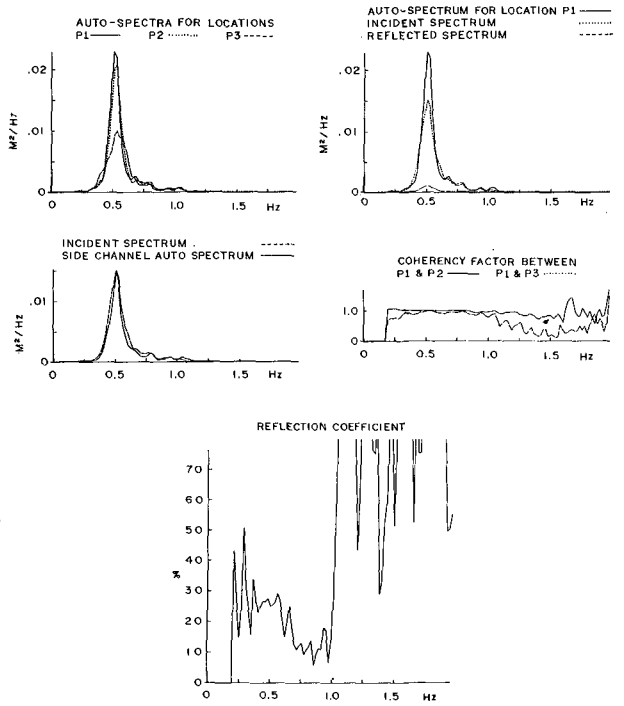

FIG.3 SEPARATION OF INCIDENT AND REFLECTED SPECTRA FOR A RUBBLE MOUND BREAKWATER (Fp = 0.51 Hz)

tern, are found to be higher than 10% for many cases of the rubble mound breakwater study.

The incident spectra calculated by the least squares method are found to agree reasonably well with the spectra measured in the side channel thereby validating this technique as a useful tool in the decomposition of the co-existing spectra.

The reflection coefficients in each band of the spectrum are presented in terms of percentage of the corresponding incident wave height. Their variations do not exhibit any specific trend with respect to frequency. It can be shown, however, that their scatter is partly due averaging applied during spectral analysis.

Downloaded from ascelibrary.org by "University of California, San Diego" on 11/17/20. Copyright ASCE. For personal use only; all rights reserved.

Downloaded from ascelibrary.org by "University of California, San Diego" on 11/17/20. Copyright ASCE. For personal use only; all rights reserved.

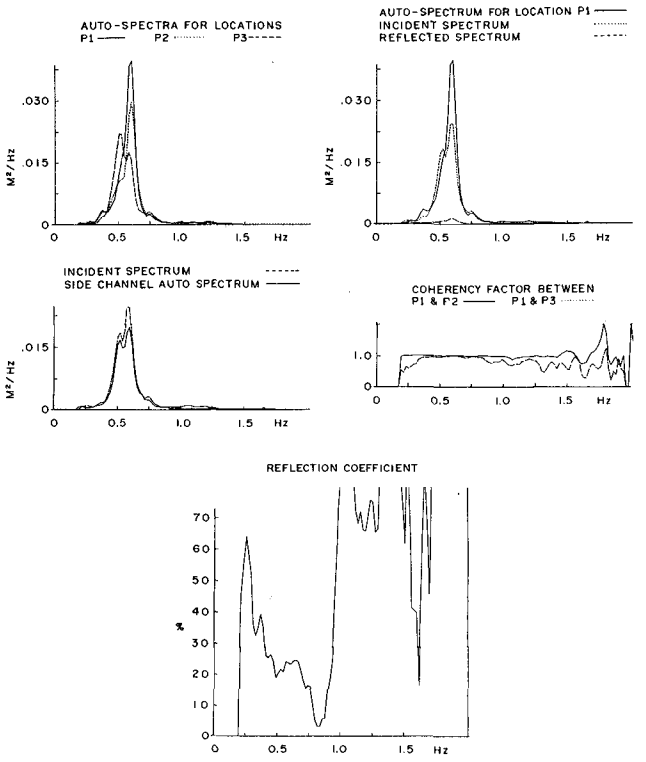

FIG.4 SEPARATION OF INCIDENT AND REFLECTED SPECTRA FOR A RUBBLE MOUND BREAKWATER (Fp = 0.60 Hz)

Another important factor worth noting is the dependency of the reflection phenomenon on wave steepness. Therefore, the reflection coefficient spectrum is highly dependent on the incident spectrum and can only be considered an average value of reflection for each frequency band over the duration of the sample record.

It must also be considered quite likely that the reflection phenomenon leads to a transfer of energy between different frequency bands and not just to its attenuation. Some incident energy at frequency f_a may therefore be radiated back at frequency f_b and appear consequently as an amplification of reflected energy at f_b.

In the range of frequencies where the incident spectrum is very low, the signal to noise ratio is very low. As a result the estimation of reflection coefficients is subject to errors and therefore produces spurious variations.

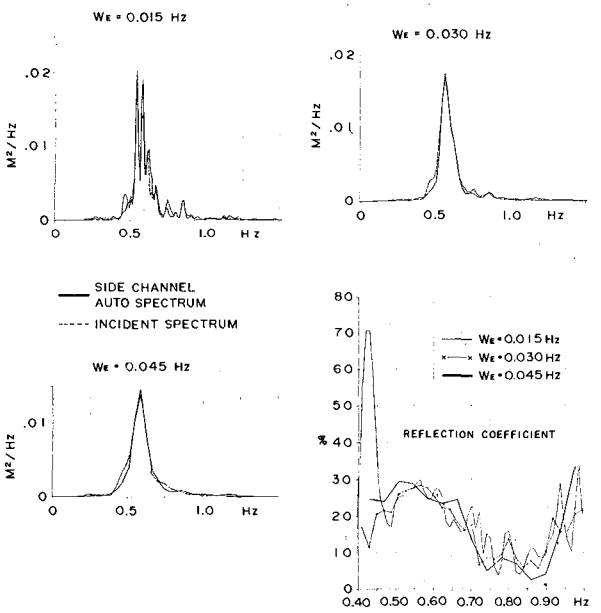

FIG.5 EFFECT ON THE CALCULATION OF REFLECTIONS DUE TO SMOOTHING WINDOW SIZE
(Fp = 0.57 Hz)

The coherency factor CF(f), presented in these figures, gives an indication of the relative phase stability in each frequency band between cross-correlated records. This is therefore a direct measure of the degree of confidence which could be attributed to the reflection coefficient in each band. When CF(f) is close to unity, the records are said to be well correlated and the opposite applies when it approaches zero. Results show that CF(f) decreases with an increase in frequency or with an increase in probe spacings. Where the spectrum has almost zero energy, CF(f) appears to exceed 1. This is clearly incorrect and can be attributed to low signal to noise ratios.

Downloaded from ascelibrary.org by "University of California, San Diego" on 11/17/20. Copyright ASCE. For personal use only; all rights reserved.

Downloaded from ascelibrary.org by "University of California, San Diego" on 11/17/20. Copyright ASCE. For personal use only; all rights reserved.

3.1 Effect of Smoothing Spectra

The smoothing of spectra in the analysis of prototype wave data is generally performed in order to improve the reliability of estimating power within a certain band of frequencies. This operation may be performed implicitly, by applying so-called "data windows" in the time domain, or explicitly, by using various frequency windows or filters in the frequency domain. In either case, the net effect is the averaging of several weighted power estimates within a frequency bandwidth defined by the particular window function chosen.

The price to be paid for improved reliability is a loss of resolution or fidelity of analysis (Jenkins and Watts, 1968). Fidelity is the ability of an analysis to reveal the true characteristics or details of a process. A low fidelity analysis would lead to a blurring or smearing of those details which may or may not be a true characteristic of the process under investigation.

The statistical techniques for the choice of window bandwidth in the analysis of prototype wave data are based on the assumption that each individual contributing component within the width of the window is a member of a stochastic process. It is important to realize that this situation does not generally apply to the analysis of wave data under laboratory conditions. If, as is usually the case, the waves were generated by some deterministic process, then the process is also deterministic in the frequency domain and the question of statistical reliability must only be answered in relation to the noise which is added to the wave data by the various mechanisms which were identified in section 2.1.

As the mixture of noise and deterministic signal is not known at this time, the question of a best choice of window bandwidth cannot be answered. Instead it may be better to experiment with different windows and compare the results. A more formal procedure along this line is known as "window closing" and is described by Jenkins and Watts (1968).

For the purpose of this report three separate explicit Hanning windows (Blackman and Tuckey, 1958) were used on laboratory generated wave data with bandwidth of 0.015, 0.03 and 0.045 Hz respectively. The results are shown in Fig. 5. The relatively small differences in results suggest that the solution is fairly stable.

Downloaded from ascelibrary.org by "University of California, San Diego" on 11/17/20. Copyright ASCE. For personal use only; all rights reserved.

3.2 Effect of Probe Spacings

Past studies using monochromatic waves (Marcou, 1969) have shown that the estimation of the incident and reflected waves are not influenced by the choice of probe spacings. However, there is one critical combination of the probe spacing for which the reflection analysis will be invalid.

The main expression used for the estimation of incident and reflected waves (Eqs. 25 and 26) will become indeterminate if its denominator D_k is equal to zero (one of these equations is given below for easy reference).

$$Z_{I,k} = \frac{1}{D_k} \cdot \left(B_{1,k} \cdot (R1+i \cdot Q1) + B_{2,k} \cdot (R2+i \cdot Q2) + B_{3,k} \cdot (R3+i \cdot Q3) \right)$$

where $D_k = 2 \cdot (\sin^2\beta_k + \sin^2\gamma_k + \sin^2(\gamma_k-\beta_k))$

D_k is equal to zero if

$$\sin\beta_k = \sin\gamma_k = \sin(\gamma_k-\beta_k) = 0$$

$$\text{or } \sin\beta_k = \sin\gamma_k = 0$$

$$\text{or } \sin\left(\frac{2\pi \cdot X12}{L_k}\right) = \sin\left(\frac{2\pi \cdot X13}{L_k}\right) = 0$$

This occurs when

$$X12 = \frac{jL_k}{2} \text{ and } X13 = \frac{m}{n} \cdot X12$$

where j, m, n and m/n are integers and L_k is the wave length for the frequency components $(k \cdot \Delta f)$ under consideration. In other words the reflection calculations become indeterminate when:

1. the distance X12 is equal to half wave length of the frequency component under consideration or even multiples of half wave length .AND.
2. the distance X13 is an integer multiple of the distance X12.

More research may be carried out to determine the optimum probe spacing for greatest accuracy and widest bandwidth. The coherency function and, perhaps the spectrum of residues as given by equation 19 could probably be used as a criterion.

On the basis of experience gained at the Hydraulics Laboratory at the National Research Council, and experiments carried out by Marcou (1969) using monochromatic waves, the following range of probe spacings are recommended:

$$X12 = L_p/10$$

$$L_p/6 < X13 < L_p/3 \quad \text{and} \quad X13 \neq L_p/5 \text{ and } \quad X13 \neq 3L_p/10$$

Another parameter which is of similar importance is the distance of probes from the reflective structure (test structure and wave paddle). It has been shown by Ishida (1972) and Goda et al (1976) that the co-existing wave height fluctuates to a certain extent near the reflective structures. However, these fluctuations become negligible beyond a distance of one wave length. Hence it is suggested that the probes be located at least one wave length (wave length corresponding to peak frequency) away from the reflective structures.

4.0 CONCLUSIONS

A satisfactory technique based on least squares analysis is described whereby the incident and reflected spectra are resolved from the measured co-existing spectra.

There is good agreement between the incident spectrum calculated by the least squares method and the corresponding spectrum measured concurrently in the side channel.

This method can be considered as superior to the 2-point method since it has:

a) wider frequency range,
b) reduced sensitivity to noise and deviations from the linear theory and,
c) lesser sensitivity to critical probe spacing.

The effect of varying the size of smoothing window in the calculation of the incident spectrum has been found to be relatively small. However a relationship between the best smoothing window and the general properties of the wave spectrum is still a subject of continuing research.

Suitable locations of probes are recommended. Probe spacings which must be avoided to eliminate singularities are also defined.

Downloaded from ascelibrary.org by "University of California, San Diego" on 11/17/20. Copyright ASCE. For personal use only; all rights reserved.

Downloaded from ascelibrary.org by "University of California, San Diego" on 11/17/20. Copyright ASCE. For personal use only; all rights reserved.

6.0 REFERENCES

1. Blackman and Tukey (1959), "The Measurement of Power Spectra from the Point of View of Communications Engineering", Dover Publications.
2. Funke, E.R. and E.P.D. Mansard (1979), "Synthesis of Realistic Sea States in a Laboratory Flume, Hydraulics Laboratory Technical Report LTR-HY-66, National Research Council, Ottawa.
3. Funke, E.R., N.L. Crookshank and M. Wingham (1980), "An Introduction to GEDAP - An Integrated Software System for Experiment Control, Data Acquisitions and Data Analysis", Proc. XXVI International Instrumentation Symposium, Seattle. (Also available as NRC Hydraulics Lab. Tech. Report LTR-HY-75.)
4. Funke, E.R. and E.P.D. Mansard (1980), "Reproduction of Prototype Random Wave Trains in a Laboratory Flume", Hydraulics Laboratory Technical Report no. LTR-HY-64, National Research Council, Ottawa (to be published).
5. Gaillard, P., M. Gauthier and F. Holly (1980), "Method of Analysis of Random Wave Experiments with Reflecting Coastal Structures", 17th International Coastal Engineering Conference, Sydney, Australia.
6. Goda, Y. and Y. Abe (1968), "Apparent Coefficient of Partial Reflection of Finite Amplitude Waves", Rep. Port and Harbour Res. Inst., Vol. 7, No. 3, pp. 3-58.
7. Goda, Y. and Y. Suzuki (1976), "Estimation of Incident and Reflected Waves in Random Wave Experiments", 15th Coastal Engineering Conference, Hawaii.
8. Ishida, A. (1972), "Transformation of Power Spectra of Wind Generated Waves Caused by Reflection", Coastal Engineering in Japan, Vol. 15, JSCE, pp. 25-33.
9. Jenkins and Watts (1968), "Spectral Analysis and Its Applications", Holden-Day.
10. Mansard, E.P.D. (1976), "Contribution à l'étude expérimentale de la propagation de la houle à travers des obstacles en forme de diaphragme", Thèse Grenoble.
11. Mansard, E.P.D. and E.R. Funke (1980), "The Measurement of Incident and Reflected Spectra Using a Least Squares Method", Hydraulics Laboratory Technical Report LTR-HY-72, National Research Council.
12. Marcou, C. (1969), "Contribution expérimentale à l'étude de la houle complexe du laboratoire", Thèse, Grenoble.
13. Morden, D.B. et al (1976), "Decomposition of Co-existing Random Wave Energy", 15th Coastal Engineering Conference, Hawaii.
14. Tadjbaksh et al (1960), "Standing Surface Waves of Finite Amplitudes", Journal of Fluid Mechanics, Vol. 8, pp. 442-451.
15. Thornton, E.B. and R.J. Calhoun (1972), "Spectral Resolution of Breakwater Reflected Waves", Journal ASCE Waterways Harbour and Coastal Engineering, WW4.